Syntheses, Crystal Structures and Optical Limiting Properties of Three Novel Organometallic Tungsten-Copper-Sulfur Clusters: $[PPh_4][(\eta^5\text{-}C_5Me_5)WS_3(CuCN)_2]$, $[(\eta^5\text{-}C_5Me_5)WS_3Cu_2(PPh_3)(\mu\text{-}CN)]_2$ and $[PPh_4][\{(\eta^5\text{-}C_5Me_5)WS_3Cu_2(CN)(Py)\}_2(\mu\text{-}CN)]$

Jian-Ping Lang,*[a,b] Qing-Feng Xu,[a] Wei Ji,[c] Hendry Izaac Elim,[c] and Kazuyuki Tatsumi[d]

Keywords: Copper / Tungsten / Sulfur / Cluster compounds

Reactions of $[PPh_4][(\eta^5\text{-}C_5Me_5)WS_3]$ with two equivalents of CuCN in MeCN produced a novel trinuclear butterfly-shaped cluster $[PPh_4][(\eta^5\text{-}C_5Me_5)WS_3(CuCN)_2]$ (**1**) in a 70% yield. Treatment of **1** with excess PPh_3 or Py gave rise to two different hexanuclear clusters $[(\eta^5\text{-}C_5Me_5)WS_3Cu_2(PPh_3)(\mu\text{-}CN)]_2$ (**2**) and $[PPh_4][\{(\eta^5\text{-}C_5Me_5)WS_3Cu_2(CN)(Py)\}_2(\mu\text{-}CN)]$ (**3**), respectively. Compounds **1**–**3** were fully characterized by spectroscopy and X-ray crystallography. The structure of the cluster anion of **1** contains a butterfly-like WS_3Cu_2 fragment in which each Cu atom is coordinated to one μ-S atom, one μ_3-S atom, and one terminal CN group. The neutral compound **2** has a double butterfly-shaped structure in which two WS_3Cu_2 fragments are interconnected by two Cu–μ-CN–Cu bridges. The anion of **3** adopts another type of double butterfly-shaped structure in which the two WS_3Cu_2 fragments are linked by a single Cu–μ-CN–Cu bridge. Compared with C_{60} in terms of the optical limiting (OL) properties measured under identical conditions, **1** and **2** exhibit a relatively good OL performance, whereas the OL effect is not observed for **3**.

Introduction

The reactions of thiomolybdates and thiotungstates $[MO_{4-n}S_n]^{2-}$ (M = Mo, W) with various transition metal halides has been extensively investigated as a result of their rich chemistry.[1−4] Their relation to industrial catalysis,[2] biological systems,[3] and electro/photonic materials has also been demonstrated.[4−5] However, only a few reactions have been reported that are involved in the utilization of metal cyanides such as CuCN and AgCN.[6] So far, a dozen Mo(W)/Cu(Ag)/S clusters containing either a terminal or bridging cyano group around their cluster framework have been prepared.[6−7] Among them, the polymeric clusters $\{[Et_4N]_2[MS_4Cu_4(CN)_4]\}_\infty$ (M = Mo, W) were reported to exhibit large optical limiting (OL) effects in DMF.[7b]

We have recently reported on a series of mixed-metal clusters prepared from the reactions of the organometallic trisulfido complex anions $[(\eta^5\text{-}C_5Me_5)MS_3]^-$ (M = Mo,[8a] W[8b]) with metal halides.[9] Intriguingly, when $[PPh_4][(\eta^5\text{-}C_5Me_5)WS_3]$ was treated with AgCN, a cyano-bridged helical polymer $\{[(\eta^5\text{-}C_5Me_5)WS_3]_2Ag_3(CN)\}_\infty$ was produced.[10] In order to extend the chemistry of $[PPh_4][(\eta^5\text{-}C_5Me_5)WS_3]$, we carried out the reaction of $[PPh_4][(\eta^5\text{-}C_5Me_5)WS_3]$ with CuCN. A discrete trinuclear anionic cluster $[PPh_4][(\eta^5\text{-}C_5Me_5)WS_3(CuCN)_2]$ (**1**) was the only product that was isolated. As discussed later in this paper, the anion of **1** contains two three-coordinate Cu atoms and two terminal CN groups. The coordination geometry around the Cu atoms may be completed, substitution of the CN groups may take place, and the formation of new clusters may be anticipated if suitable donor ligands are used. In this context, the reactions of **1** with excess PPh_3 or Py were performed, and two novel hexanuclear cyano-bridged clusters $[(\eta^5\text{-}C_5Me_5)WS_3Cu_2(PPh_3)(\mu\text{-}CN)]_2$ (**2**) and $[PPh_4][\{(\eta^5\text{-}C_5Me_5)WS_3Cu_2(CN)(Py)\}_2(\mu\text{-}CN)]$ (**3**) were obtained. Furthermore, in our continued efforts to search for good OL materials,[5a−5c] we have also examined the OL properties of **1**−**3** in solution with 7-ns laser pulses at 532 nm. Herein we report on the syntheses and crystal structures of **1**−**3**, along with their OL properties in solution.

[a] School of Chemistry and Chemical Engineering, Suzhou University,
Suzhou, 215006, P. R. China
Fax: (internat.) + 86-512-65224783
E-mail: jplang@suda.edu.cn
[b] State Key Laboratory of Coordination Chemistry, Nanjing University,
Nanjing, 210093, P. R. China
[c] Department of Physics, National University of Singapore,
2 Science Drive 3, 117542 Singapore
[d] Research Center for Materials Science, and Department of Chemistry, Graduate School of Science, Nagoya University,
Furo-cho, Chikusa-ku, Nagoya 464-8602, Japan

  DOI: 10.1002/ejic.200300204

Results and Discussion

Synthesis and Spectral Characterization

As depicted in Scheme 1, addition of 2 equiv. of CuCN to a red solution of $[PPh_4][(\eta^5\text{-}C_5Me_5)WS_3]$ in MeCN generated a darkened solution, which was stirred for 1 h and filtered. The filtrate was layered with Et_2O, affording $[PPh_4][(\eta^5\text{-}C_5Me_5)WS_3(CuCN)_2]$ (**1**) as red crystals in a 70% yield. Treatment of **1** in MeCN with excess PPh_3 or Py resulted in a homogeneous solution. Subsequent standard workups produced two new clusters, $[(\eta^5\text{-}C_5Me_5)WS_3Cu_2(\mu\text{-}CN)(PPh_3)]_2$ (**2**) as red plates, and $[PPh_4][\{(\eta^5\text{-}C_5Me_5)WS_3Cu_2(CN)(Py)\}_2(\mu\text{-}CN)]$ (**3**) as orange-red needles, respectively. Compounds **1**−**3** are relatively air and moisture stable in the solid state. Compounds **1** and **3** are soluble in DMF and slightly soluble in MeCN. Both **1** and **3** are insoluble in CH_2Cl_2 and $CHCl_3$. Compound **2** dissolves in CH_2Cl_2 and $CHCl_3$, and not in MeCN and DMF.

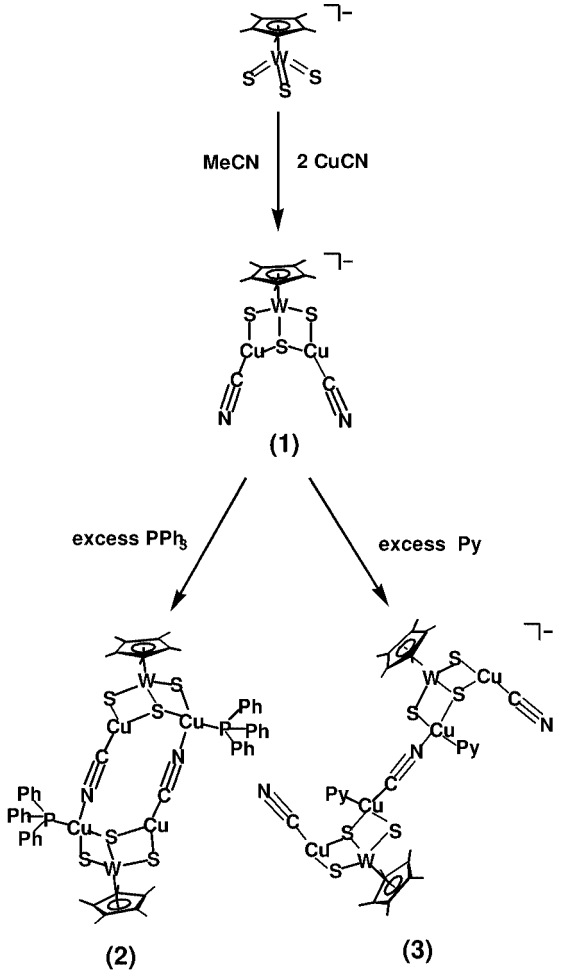

Scheme 1

The FT-IR spectra of **1**−**3** display bands assigned to the W−S_{br} stretching vibrations at 433/410 (**1**), 434/417/409 (**2**) and 445/430/413 (**3**) cm^{-1}, respectively. The IR spectrum of **1** shows a strong terminal C≡N stretching vibration at 2119 cm^{-1}, while that of **2** shows a bridging C≡N stretching vibration at 2139 cm^{-1}. Compound **3** exhibits both a terminal C≡N stretching vibration at 2053 cm^{-1} and a bridging C≡N stretching vibration at 2130 cm^{-1}. The ^1H NMR spectra of **1** and **3** in CD_3CN and of **2** in $CDCl_3$ at ambient temperature display a single resonance assigned to the $\eta^5\text{-}C_5Me_5$ group at 2.05 (**1**), 2.05 (**2**), and 2.08 (**3**) ppm, respectively. The UV/Vis spectra of **1** in MeCN and of **3** in DMF are characterized by three bands at 435, 390, and 214 nm (**1**), 452, 393, and 321 nm (**3**), while that of **2** in CH_2Cl_2 exhibits only one absorbance band at 394 nm. As the electronic spectrum of $[PPh_4][(\eta^5\text{-}C_5Me_5)WS_3]$ in MeCN shows a strong absorbance band at 381 nm,[8b] the bands at 390 (**1**), 394 (**2**), and 393 (**3**) nm observed in the UV/Vis spectra of **1**, **2**, and **3** are red-shifted (Figure 1), and they are probably dominated by the S→W^{VI} charge-transfer transitions of the $(\eta^5\text{-}C_5Me_5)WS_3$ moiety.[9c] The crystal structures of **1**−**3** were further confirmed by single crystal X-ray analysis.

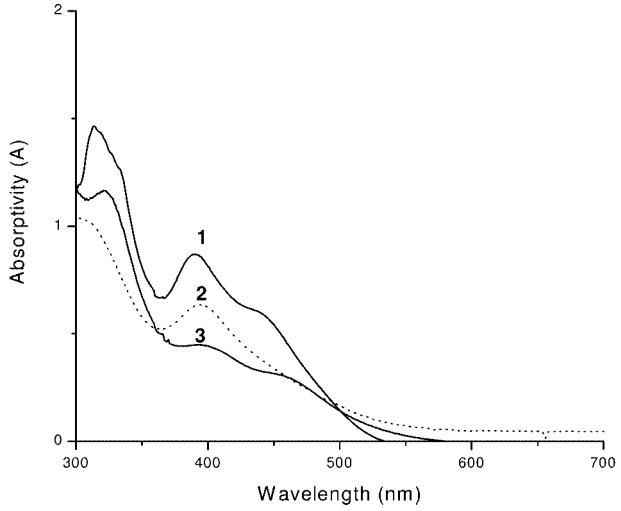

Figure 1. Absorbance spectra of **1** in MeCN, **2** in CH_2Cl_2, and **3** in DMF with a 1-mm optical length

Crystal Structure of $[PPh_4][(\eta^5\text{-}C_5Me_5)WS_3(CuCN)_2]$ (1)

Compound **1**·MeCN crystallizes in the orthorhombic space group $Pna2_1$ and the asymmetric unit contains one discrete anion $[(\eta^5\text{-}C_5Me_5)WS_3(CuCN)_2]^-$, one $[PPh_4]^+$ cation, and one MeCN solvated molecule. The $[PPh_4]^+$ cation does not interact with the cluster anion and all the bond lengths and angles related to this cation are typical. Therefore, Figure 2 only shows the structure of the cluster anion of **1**, and Table 1 lists the selected bond lengths and angles of the cluster anion of **1**. The cluster anion of **1** consists of a $(\eta^5\text{-}C_5Me_5)WS_3$ unit bound to two CuCN groups via one μ_3-S and two μ-S atoms. Alternatively, the anion of **1** may be described as containing a butterfly-shaped WS_3Cu_2 fragment, which has previously been observed in $[MoOS_3(CuSPh)_2]^{2-}$,[6a] $[(\eta^5\text{-}C_5Me_5)WS_3Cu_2(PPh_3)_2Br]$,[9d] $[MoOS_3M'_2(PPh_3)_3]$ (M = W, Mo; M′ = Cu^I, Ag^I),[11a,11b] and $[WS_4Cu_2(dppm)_3]$.[11c] The $(\eta^5\text{-}C_5Me_5)WS_3$ unit of **1** has a slightly distorted three-legged piano stool structure. The mean W−μ-S and W−μ_3-S bond lengths, 2.237 Å and 2.308 Å, are elongated by 0.05 Å and 0.12 Å, respectively,

relative to that of $[PPh_4][(\eta^5\text{-}C_5Me_5)WS_3]$,[8b] due to the coordination of the sulfur atoms to the Cu atoms. Each Cu atom adopts a trigonal planar geometry, coordinated by one μ-S atom, one μ_3-S atom, and one terminal CN group. The mean W···Cu distance of 2.660 Å is similar to those found in the three-coordinate Cu clusters such as $[PPh_4]_2[(\eta^5\text{-}C_5Me_5)WS_3Cu_3Br_3]_2$ (2.661 Å)[9a] and $[PPh_4][\{(\eta^5\text{-}C_5Me_5)WS_3Cu_2\}_2S_2]_2$ (2.677 Å).[12] The average Cu−S length of 2.230 Å is similar to those of $[PPh_4]_2[(\eta^5\text{-}C_5Me_5)WS_3Cu_3Br_3]_2$ (2.234 Å) and $[PPh_4][\{(\eta^5\text{-}C_5Me_5)WS_3Cu_2\}_2S_2]_2$ (2.222 Å). The average terminal Cu−C length (1.892 Å) in **1** compares with those found in $[n\text{-}Pr_4N]_2[MoS_4(CuCN)]$ (1.880 Å) and $[AsPh_4]_2[MoS_4(\text{-}CuCN)_2]$ (1.886 Å).[6c]

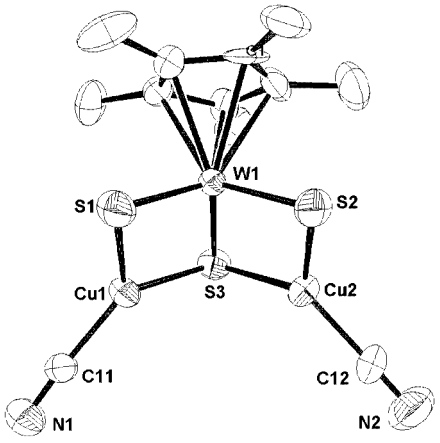

Figure 2. The perspective view of the anion of **1**. The thermal ellipsoids are drawn at the 50% probability level and the hydrogen atoms are omitted for clarity

Table 1. Selected bond lengths [Å] and angles [°] of **1**

W(1)···Cu(1)	2.6556(14)	W(1)···Cu(2)	2.6765(14)
W(1)−S(1	2.210(3)	W(1)−S(2)	2.263(3)
W(1)−S(3)	2.308(2)	Cu(1)−S(1)	2.211(3)
Cu(1)−S(3)	2.250(3)	Cu(2)−S(3)	2.226(3)
Cu(2)−S(2)	2.212(3)	Cu(1)−C(11)	1.88(1)
Cu(2)−C(12)	1.903(12)	N(1)−C(11)	1.148(13)
N(2)−C(12)	1.113(15)		
Cu(1)···W(1)···Cu(2)	78.47(4)	S(1)−W(1)−S(2)	104.29(13)
S(1)−W(1)−S(3)	106.4(1)	S(2)−W(1)−S(3)	104.8(1)
S(1)−Cu(1)−S(3)	108.4(1)	S(1)−Cu(1)−C(11)	124.9(3)
S(3)−Cu(1)−C(11)	126.7(3)	S(2)−Cu(2)−S(3)	109.31(11)
S(2)−Cu(2)−C(12)	122.4(4)	S(3)−Cu(2)−C(12)	128.2(4)
Cu(1)−N(1)−C(11)	175.0(10)	Cu(2)−C(12)−N(2)	177.5(13)
Cu(1)−S(3)−Cu(2)	97.3(1)		

Crystal Structures of $[(\eta^5\text{-}C_5Me_5)WS_3Cu_2(PPh_3)(\mu\text{-}CN)]_2$ (2) and $[PPh_4][\{(\eta^5\text{-}C_5Me_5)WS_3Cu_2(CN)(Py)\}_2(\mu\text{-}CN)]$ (3)

Compound **2** crystallizes in the monoclinic space group $P2_1/n$ and the asymmetric unit contains half a molecule of $[(\eta^5\text{-}C_5Me_5)WS_3Cu_2(PPh_3)(\mu\text{-}CN)]_2$; **3**·1.25Py crystallizes in the triclinic space group $P\bar{1}$ and the asymmetric unit consists of one discrete $[\{(\eta^5\text{-}C_5Me_5)WS_3Cu_2(CN)(Py)\}_2(\mu\text{-}CN)]^-$ anion, one $[PPh_4]^+$ cation, and 1.25 molecules of pyridine as solvated molecules. The refinements of the structures of **2** and **3** showed that the bridging cyanide groups between the Cu atoms have two orientations (i.e. the bridging cyanide groups are either coordinated through the C atoms, or through the N atoms). All the relevant C and N atoms were refined with a 50% probability of being C or N over each orientation. The derived Cu−C and Cu−N distances at the same site [e.g. Cu(1)−C(1) and Cu(1)−N(1a) in **2**, and Cu(1)−N(2) and Cu(1)−C(26a) in **3**] are identical and really express the average value. It is not known whether the distances in an ordered system would be equal. Therefore, Figure 3 shows the structure of **2** with the orientation of the bridging cyanide containing C(1) and N(1), while Figure 4 depicts the perspective view of the $[\{(\eta^5\text{-}C_5Me_5)WS_3Cu_2(CN)(Py)\}_2(\mu\text{-}CN)]^-$ anion of **3** with

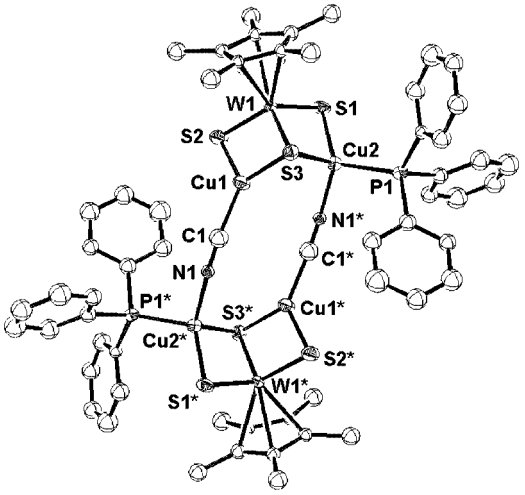

Figure 3. The perspective view of the molecular structure of **2** with 50% thermal ellipsoids. The C and N atoms of the bridging cyanide are disordered and only one orientation [C(1) and N(1)] is shown, and the hydrogen atoms are omitted for clarity.

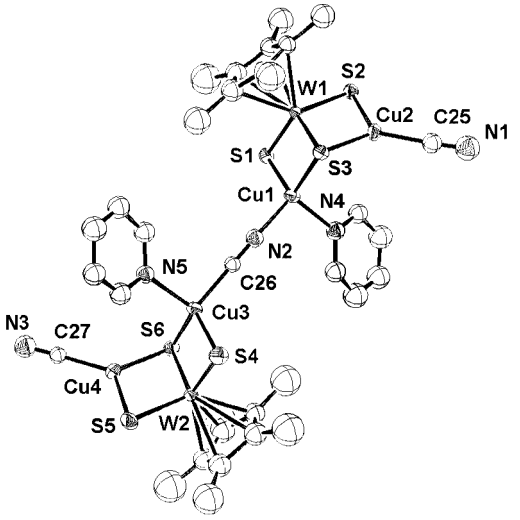

Figure 4. The perspective view of the anion of **3** with 50% thermal ellipsoids. The C and N atoms of the bridging cyanide are disordered and only one orientation [C(26) and N(2)] is shown, and the hydrogen atoms are omitted for clarity.

Table 2. Selected bond lengths [Å] and angles [°] of **2**

W(1)···Cu(1)	2.657(2)	W(1)···Cu(2)	2.768(2)
W(1)−S(1)	2.220(4)	W(1)−S(2)	2.229(5)
W(1)−S(3)	2.291(4)	Cu(1)−S(2)	2.199(5)
Cu(1)−S(3)	2.219(5)	Cu(1)−C(1)	1.919(10)
Cu(2)−S(1)	2.272(5)	Cu(2)−S(3)	2.314(5)
Cu(2*)−N(1)	2.040(9)	Cu(2)−P(1)	2.251(5)
N(1)−C(1)	1.135(12)		
Cu(1)···W(1)···Cu(2)	70.12(6)	S(1)−W(1)−S(2)	105.3(2)
S(1)−W(1)−S(3)	104.6(2)	S(2)−W(1)−S(3)	105.1(2)
S(2)−Cu(1)−S(3)	108.6(2)	S(2)−Cu(1)−C(1)	120.5(3)
S(3)−Cu(1)−C(1)	130.9(3)	S(1)−Cu(2)−S(3)	102.2(2)
S(1)−Cu(2)−P(1)	117.8(2)	S(3)−Cu(2)−P(1)	108.4(2)
S(3)−Cu(2)−N(1*)	108.80(13)	P(1)−Cu(2)−N(1*)	103.9(2)
S(1)−Cu(2)−N(1*)	115.5(2)	Cu(1)−S(3)−Cu(2)	86.9(2)
Cu(1)−C(1)−N(1)	170.9(8)	Cu(2*)−N(1)−C(1)	160.7(7)

Table 3. Selected bond lengths [Å] and angles [°] of **3**

W(1)···Cu(1)	2.711(2)	W(1)···Cu(2)	2.657(2)
W(2)···Cu(3)	2.716(2)	W(2)···Cu(4)	2.664(2)
W(1)−S(1)	2.218(4)	W(1)−S(2)	2.231(3)
W(1)−S(3)	2.290(4)	W(2)−S(4)	2.221(4)
W(2)−S(5)	2.235(3)	W(2)−S(6)	2.295(4)
Cu(1)−S(1)	2.259(4)	Cu(1)−S(3)	2.265(4)
Cu(1)−N(2)	1.939(7)	Cu(1)−N(4)	2.11(2)
Cu(2)−S(2)	2.209(4)	Cu(2)−S(3)	2.216(4)
Cu(2)−C(25)	1.89(2)	Cu(3)−S(4)	2.265(5)
Cu(3)−S(6)	2.262(4)	Cu(3)−C(26)	1.945(8)
Cu(3)−N(5)	2.165(13)	Cu(4)−S(5)	2.202(5)
Cu(4)−S(6)	2.219(4)	Cu(4)−C(27)	1.90(2)
N(1)−C(25)	1.14(2)	N(2)−C(26)	1.154(11)
N(3)−C(27)	1.12(2)		
Cu(1)···W(1)···Cu(2)	77.89(6)	Cu(3)···W(2)···Cu(4)	76.77(6)
S(1)−W(1)−S(2)	104.3(1)	S(1)−W(1)−S(3)	106.4(1)
S(2)−W(1)−S(3)	105.35(13)	S(4)−W(2)−S(5)	104.9(2)
S(5)−W(2)−S(6)	104.9(1)	S(4)−W(2)−S(6)	106.2(2)
S(1)−Cu(1)−S(3)	105.9(2)	S(1)−Cu(1)−N(2)	115.8(2)
S(3)−Cu(1)−N(2)	115.8(2)	S(1)−Cu(1)−N(4)	102.8(4)
S(3)−Cu(1)−N(4)	113.4(4)	N(2)−Cu(1)−N(4)	102.6(4)
S(2)−Cu(2)−S(3)	108.7(2)	S(2)−Cu(2)−C(25)	122.0(5)
S(3)−Cu(2)−C(25)	129.1(5)	S(4)−Cu(3)−S(6)	105.9(2)
S(4)−Cu(3)−N(5)	101.3(4)	S(6)−Cu(3)−N(5)	115.4(3)
S(4)−Cu(3)−C(26)	117.2(3)	S(6)−Cu(3)−C(26)	114.1(2)
N(5)−Cu(3)−C(26)	102.6(5)	S(5)−Cu(4)−S(6)	108.6(2)
S(5)−Cu(4)−C(27)	123.9(5)	S(6)−Cu(4)−C(27)	127.4(5)
Cu(1)−S(3)−Cu(2)	97.7(2)	Cu(4)−S(6)−Cu(3)	96.4(2)
Cu(1)−N(2)−C(26)	179.0(6)	Cu(2)−C(25)−N(1)	177.0(17)
Cu(3)−C(26)−N(2)	179.4(7)	Cu(4)−C(27)−N(3)	178.3(15)

the orientation of the bridging cyanide containing C(26) and N(2). Tables 2 and 3 list the selected bond lengths and angles for **2** and **3** with the orientation of the bridging cyanide consisting of C(1) and N(1) in **2**, and C(26) and N(2) in **3**, respectively. The molecular structure of **2** can be viewed as a double butterfly-shaped structure in which two [(η^5-C_5Me_5)WS_3Cu_2] fragments are interconnected by a pair of Cu−μ-CN−Cu bridges. Meanwhile, the anion of **3** presents another type of double butterfly-shaped structure in which two [(η^5-C_5Me_5)WS_3Cu_2] fragments are linked by a single Cu−μ-CN−Cu bridge. To the best of our knowledge, the two structures are unprecedented in the tetrathiometallates. In both structures, each [(η^5-C_5Me_5)WS_3Cu_2] fragment shows a very similar structure to that of **1**. However, the two Cu atoms in each [(η^5-C_5Me_5)WS_3Cu_2] fragment of **2** and **3** exhibit a somewhat different coordination geometry from that of **1**. One Cu atom adopts a similar trigonal planar geometry, while the other Cu atom is coordinated by two S atoms, one CN group and one PPh_3 (**2**) or Py (**3**) group, thus exhibiting a distorted tetrahedral coordination geometry. Therefore, the different coordination geometries around the Cu atoms results in different W···Cu distances within the same [(η^5-C_5Me_5)WS_3Cu_2] fragment. The mean W···Cu distances for the three-coordinate Cu atom [2.657(2) Å in **2** and 2.661(2) Å in **3**] are similar to that of **1**. However, the mean W···Cu distance for the four-coordinate Cu atom in **2** [2.768(2) Å] is similar to those of [WS_4Cu_4(dppm)$_4$](PF_6)$_2$ (2.760 Å),[11c] but longer than those found in **3** [2.714(2) Å] and other clusters containing tetrahedral Cu atoms such as [(η^5-C_5Me_5)WS_3-Cu_2(PPh_3)$_2$Br] (2.704 Å),[9d] [Et_4N]$_2$[WS_4Cu_4(NCS)$_4$] (2.691 Å),[13a] [Et_4N]$_4$[$WS_4Cu_4I_6$] (2.692 Å),[13b] and [WS_4Cu_4(γ-MePy)$_8$][W_6O_{19}] (2.686 Å).[13c] The mean Cu−μ_3-S−Cu angle of 97.1(2)° in **3** is similar to that of **1**; however, it is about 10° smaller than that in **2**. The reason may be ascribed to the larger steric bulk of the two PPh_3 ligands coordinated at Cu(2) and Cu(2*) in **2**. The effect is also reflected in the linearity of the Cu−μ-CN−Cu bridges of **2** and **3**. The Cu−μ-CN−Cu portion in **2** is slightly bent, with Cu(1)−C(1)−N(1) and C(1)−N(1)−Cu(2*) angles of 170.9(8)° and 160.7(7)°, respectively. However, the Cu−μ-CN−Cu bridge in **3** is practically linear, with Cu(1)−N(2)−C(26) and Cu(3)−C(26)−N(2) angles of 179.0(6)° and 179.4(7)°, respectively. The Cu−C/N and Cu−N/C distances of the bridging cyanide groups in **2** and **3** range from 1.910(6) Å to 2.048(14) Å, which are similar to those found in [Cu(4-CNPy)(μ-CN)] [Cu−N/C = 1.907(2) Å and Cu−C/N = 1.999(2) Å].[13d] The mean Cu−P length of 2.251(5) Å in **2** is similar to those found in [(η^5-C_5Me_5)WS_3Cu_3(PPh_3)$_2$Br$_2$] (2.247 Å) and [PPh_4][(η^5-C_5Me_5)$WS_3Cu_3Br_3$(dppm)] (2.270 Å).[9c] The mean Cu−N(Py) length of 2.138 Å in **3** is longer than those found in [WS_4Cu_4(γ-MePy)$_8$][W_6O_{19}] (2.02 Å)[13c] and [Cu(Py)$_4$]-ClO_4 (2.046 Å).[14] The mean W−μ-S, W−μ_3-S, and Cu−S distances in both **2** and **3** compare with those found in **1**.

Optical Limiting (OL) Properties of 1−3

As shown in Figure 1, compounds **1**−**3** have a low absorbance at 532 nm. This promises low intensity loss and small temperature changes by photon absorption when the laser pulse propagates in these materials. The fluence-dependent transmission measurements of **1**−**3** are depicted in Figure 5. For **1**, the light energy transmitted begins to deviate from normal linear behavior as soon as the input light fluence reaches about 0.4 J/cm^2, and the material becomes increasingly less transparent as the light fluence rises. We define the limiting threshold as the incident fluence at which the sample transmittance falls to 50% of the corresponding linear transmittance. The limiting threshold of

compound **1** is 7.5 J/cm^2. For **2**, when the input light fluence reaches about 2.6 J/cm^2, the light energy transmitted begins show less than linear behavior. The limiting threshold for compound **2** is larger than 10 J/cm^2. Unfortunately, no OL effects are observed for compound **3**. Although the concentration of C_{60} ($9.02\cdot10^{-4}$ M) is higher than the concentrations of **1** ($3.57\cdot10^{-4}$ M) and **2** ($1.20\cdot10^{-4}$ M), the OL performance of **1** is about 3 times better than that of C_{60} measured under identical conditions, while the OL performance of compound **2** is similar to C_{60}. The poor solubility of compounds **1** and **2** prohibits higher concentrations to be attained, and hence limits their OL performance. Better OL effects would be expected for higher concentrations of these compounds.

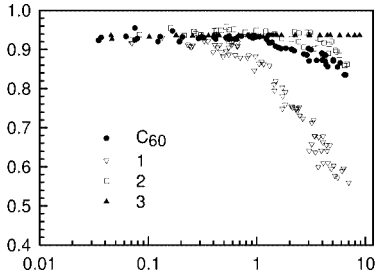

Figure 5. Optical limiting responses to 7-ns, 532 nm laser pulses, of **1** in MeCN, **2** in CH_2Cl_2, **3** in DMF, and C_{60} in toluene. Solutions with 92% transmittance at 532 nm correspond to $3.57\cdot10^{-4}$ M (**1**), $1.20\cdot10^{-4}$ M (**2**), $1.69\cdot10^{-4}$ M (**3**), and $9.02\cdot10^{-4}$ M (C_{60}), respectively

Conclusion

We demonstrated the facile synthesis of **1** and its reactivity towards PPh_3 and Py. The successful isolation of **2** and **3** shows that compound **1** can be a useful precursor for the construction of new W−Cu−S clusters in the presence of suitable donor ligands. The structures of **1**−**3** have been fully characterized by spectroscopy and X-ray analysis. Compounds **2** and **3** exhibit two types of double butterfly-shaped structures, which have not previously been observed in the chemistry of the corresponding tetrathiometallates. The OL properties of **1**−**3** in solution have been measured, and **1** and **2** exhibit relatively good OL performances when compared with C_{60}. As some preformed clusters may be assembled into supramolecular compounds via the bridging ligands such as 4,4′-bipy, and their NLO performances may be improved,[15] it is still worth screening more compounds formed from the reactions of **1** with hooking ligands such as the one mentioned above. We are currently investigating this.

Experimental Section

General: All manipulations were carried out under argon using standard Schlenk-techniques. $[PPh_4][(\eta^5\text{-}C_5Me_5)WS_3]$ was prepared as reported previously.[8b] Other chemicals were obtained from commercial sources and used as received. All solvents were predried over activated molecular sieves and refluxed over the appropriate drying agents under argon. The IR spectra were recorded on a Nicolet MagNa-IR500 FT-IR spectrometer (4000−400 cm^{-1}). ^{1}H NMR spectra were recorded at ambient temperature on a Varian UNITYplus-400 spectrometer. UV/Vis spectra were measured on a Hitachi UV-3410 spectrophotometer. The elemental analyses for C, H, and N were performed on a Carlo−Erba CHNO-S microanalyzer.

Reaction of $[PPh_4][(\eta^5\text{-}C_5Me_5)WS_3]$ with CuCN: CuCN (0.023 g, 0.26 mmol) was added to a red solution of $[PPh_4][(\eta^5\text{-}C_5Me_5)WS_3]$ (0.10 g, 0.13 mmol) in MeCN (10 mL). The solution quickly turned dark red and the mixture was stirred at room temperature for 1 h and then filtered. Diethyl ether (20 mL) was carefully layered onto the filtrate, forming red prisms of $[PPh_4][(\eta^5\text{-}C_5Me_5)WS_3(CuCN)_2]\cdot$MeCN (**1**·MeCN), which were isolated by filtration, washed with Et_2O, and dried in vacuo. Yield: 0.085 g (70%). $C_{36}H_{35}Cu_2N_2PS_3W$: calcd. C 47.02, H 4.51, N 4.49; found C 46.78, H 3.90, N 4.31%. UV/Vis (MeCN) [λ_{max}/nm (ε/M^{-1}cm^{-1})]: 435 (1700), 390 (6300), 314 (8600). IR (KBr disk): $\tilde{\nu}$ = 2119 (s), 1586 (s), 1483 (s), 1439 (vs), 1377 (m), 1318 (w), 1186 (w), 1109 (vs), 1025 (m), 995 (m), 754 (s), 724 (vs), 692 (s), 531 (s), 433 (w), 410 (m) cm^{-1}. ^{1}H NMR (CD_3CN, 400 MHz, 25 °C): δ = 7.26−7.89 (m, 20 H, PPh_4^+), 2.05 (s, 5 H, $\eta^5\text{-}C_5Me_5$) ppm.

Reaction of 1 with PPh_3: Treatment of a solution of **1** (0.042 g, 0.05 mmol) in MeCN (5 mL) with PPh_3 (0.026 g, 0.1 mmol) gave rise to a homogeneous solution, which was allowed to stir for 30 min. Diethyl ether (5 mL) was carefully layered onto the filtrate, forming red plates of $[(\eta^5\text{-}C_5Me_5)WS_3Cu_2(\mu\text{-}CN)(PPh_3)]_2$ (**2**), which were isolated by filtration, washed with Et_2O, and dried in vacuo. Yield: 0.071 g (85%). $C_{29}H_{30}Cu_2NPS_3W$: calcd. C 41.53, H 4.01, N 1.75; found C 41.89, H 3.90, N 1.68%. IR (KBr disk): $\tilde{\nu}$ = 2139 (s), 1480 (m), 1435 (s), 1376 (m), 1097 (m), 1027 (m), 747 (s), 723 (w), 695 (vs), 518 (s), 434 (m), 417 (w), 409 (w) cm^{-1}. UV/Vis (CH_2Cl_2) [λ_{max}/nm (ε/M^{-1}cm^{-1})]: 394 (5600). ^{1}H NMR ($CDCl_3$, 400 MHz, 25 °C): δ = 7.27−7.89 (m, 15 H, PPh_3), 2.05 (s, 5 H, $\eta^5\text{-}C_5Me_5$) ppm.

Reaction of 1 with Py: Compound **1** (0.042 g, 0.05 mmol) was dissolved in 1.5 mL of pyridine. The mixture was stirred at room temperature for 30 min, giving a clear solution. Diethyl ether (5 mL) was carefully layered onto the filtrate to form orange-red needles of $[PPh_4][\{(\eta^5\text{-}C_5Me_5)WS_3Cu_2(CN)(Py)\}_2(\mu\text{-}CN)]\cdot1.25$Py (**3**·1.25Py), which were isolated by filtration, washed with Et_2O, and dried in vacuo. Yield: 0.063 g (80%). $C_{29}H_{30}Cu_2NPS_3W$: calcd. C 48.42, H 4.50, N 4.12; found C 48.18, H 4.21, N 3.97%. IR (KBr disk): $\tilde{\nu}$ = 2130 (m), 2053 (m), 1483 (m), 1436 (s), 1376 (m), 1108 (vs), 996 (m), 753 (m), 724 (vs), 690 (vs), 527 (vs), 445 (w), 430 (w), 413 (w) cm^{-1}. UV/Vis (DMF) [λ_{max}/nm (ε/M^{-1}cm^{-1})]: 452 (20200), 393 (7700), 321 (5400). ^{1}H NMR ($CDCl_3$, 400 MHz, 25 °C): δ = 8.62 (br. s, 2 H, Py), 7.64−7.90 (m, 28 H, Py+PPh_4^+), 2.08 (s, 5 H, $\eta^5\text{-}C_5Me_5$) ppm.

X-ray Diffraction Crystallography: All measurements were performed on a Rigaku Mercury CCD X-ray diffractometer (3 kV, sealed tube) at −80 °C, using graphite monochromated Mo-*Kα* (λ = 0.71070 Å). A red chip of **1**·MeCN with dimensions 0.60 × 0.40 × 0.20 mm, a red prism of **2** with dimensions 0.10 × 0.05 × 0.05 mm, and a red platelet of **3**·1.25Py with dimensions 0.55 × 0.15 × 0.05 mm, were mounted at the top of a glass fiber. Diffraction data were collected at ω mode with a detector distance of 55 mm (**1**·MeCN and **2**) or 35 mm (**3**·1.25Py) to the crystal. Indexing was performed from 6 images, each of which was exposed for 15 s. A total of 1080 (**1**·MeCN) or 720 (**2** and **3**·1.25Py) oscillation images were collected in the range $1.95° < 2\theta < 54.96°$ for

Table 4. Summary of the crystal data for the structures of **1**·MeCN, **2**, and **3**·1.25Py

	1·MeCN	**2**	**3**·1.25Py
Empirical formula	$C_{38}H_{38}Cu_2N_3PS_3W$	$C_{58}H_{60}Cu_4N_2P_2S_6W_2$	$C_{63.25}H_{66.25}Cu_4N_{6.25}PS_6W_2$
F_w	974.83	1661.32	1575.38
Crystal system	Orthorhombic	monoclinic	triclinic
Space group	$Pna2_1$	$P2_1/n$	$P\bar{1}$
a [Å]	33.919(8)	12.199(2)	9.215(1)
b [Å]	7.626(2)	15.248(3)	17.811(3)
c [Å]	15.342(3)	16.173(3)	20.900(4)
α [°]			88.383(9)
β [°]		91.879(9)	82.249(9)
γ [°]			80.901(8)
V [Å^3]	3968.6(15)	3006.9(10)	3356.0(10)
Z	4	2	2
D_c [g cm^{-3}]	1.631	1.835	1.559
μ [mm^{-1}]	4.185	5.504	3.209
Reflections [$I>3.00\sigma(I)$]	3670	2220	8875
Parameters	456	210	583
R[a]	0.032	0.043	0.058
R_w[b]	0.049	0.044	0.069
GOF[c]	1.144	0.962	1.474
Largest residual peaks and hole [e·Å^{-3}]	0.80 and −0.81	0.92 and −1.15	1.84 and −1.41

[a] $R = \Sigma F_o| - |F_c\|/\Sigma|F_o|$. [b] $R_w = \{w\Sigma(|F_o| - |F_c|)^2/\Sigma w|F_o|^2\}^{1/2}$. [c] GOF $= \{\Sigma w(|F_o| - |F_c|)^2/(M - N)\}^{1/2}$, where M is the number of reflections and N is the number of parameters.

1·MeCN, $1.97° < 2\theta < 50.04°$ for **2**, and $1.60° < 2\theta < 61.86°$ for **3**·1.25Py. The collected data were reduced by using the program CrystalClear (Rigaku and MSC, Ver. 1.3, 2001), and an empirical absorption correction was applied which resulted in transmission factors ranging from 0.266 to 0.433 for **1**·MeCN, from 0.610 to 0.759 for **2**, and from 0.623 to 0.852 for **3**·1.25Py. The reflection data were also corrected for Lorentz and polarization effects.

The structures of **1**·MeCN and **2** were solved by direct methods[16a] while that of **3**·1.25Py by heavy-atom Patterson methods,[16b] and expanded using Fourier techniques.[16c] For **1**·MeCN, all non-hydrogen atoms except those of the MeCN crystal solvent molecule were refined anisotropically. For **2**, W, Cu, S, and P atoms were refined anisotropically, while C and N atoms were refined isotropically. In both cases, all hydrogen atoms were introduced at the calculated positions and included in the structure-factor calculations. Crystal **3**·1.25Py contains 1.25 Py solvated molecules in an asymmetric unit. One Py solvent molecule is refined isotropically. The other is located on a center of symmetry and is refined with one-quarter occupancy. All non-H atoms except those of CN, Py, and η^5-C_5Me_5 were refined anisotropically. Hydrogen atoms except those of the two Py solvent molecules were placed on the idealized positions and included in the final structure-factor refinements. In the structure of **2** or **3**·1.25Py, the orientation of the bridging cyanide group was found to be disordered, and the C and N atoms were refined with a 50% probability of being C or N, i.e. C(1)/N(1a) = 0.5:0.5 and N(1)/C(1a) = 0.5:0.5 (**2**), C(26)/N(2a) = 0.5:0.5, and N(2)/C(26a) = 0.5:0.5 (**3**·1.25Py). Neutral atom scattering factors were taken from Cromer and Waber.[17a] Anomalous dispersion effects were included in $F_{calcd.}$.[17b] All calculations were performed on a Dell workstation using the CrystalStructure crystallographic software package (Rigaku and MSC, Ver. 3.0, 2002). A summary of the key crystallographic information for **1**·MeCN, **2**, and **3**·1.25Py is given in Table 4. CCDC-202420 (**1**), 202421 (**2**), and 202422 (**3**) contain the supplementary crystallographic data for this paper. These data can be obtained free of charge at http://www.ccdc.cam.ac.uk/retrieving.html [or from the Cambridge Crystallographic Data Centre, 12 Union Road, Cambridge CB2 1EZ, UK; Fax: (internat.) + 44-1223/336-033; E-mail: deposit@ccdc.cam.ac.uk].

Optical Limiting Measurements: Samples were dissolved in MeCN (**1**), CH_2Cl_2 (**2**), and DMF (**3**). The solutions with concentrations of $3.57\cdot10^{-4}$ M (**1**), $1.20\cdot10^{-4}$ M (**2**), and $1.69\cdot10^{-4}$ M (**3**) were contained in a 1-mm-thick quartz cuvette. Optical limiting experiments were performed with a Q-switched, frequency-doubled Nd:YAG laser (λ = 532 nm) with linearly polarized 7-ns pulses. The interval between the laser pulses was set at 10 s so that every pulse of light was assured to meet fresh molecules in the sample to eliminate the influence of any photo-degradation. The optical limiting phenomenon was demonstrated by measuring fluence-dependent transmissions. The laser pulses were focused on to the sample using a focusing mirror of 25-cm focal length. The spot radius of the laser pulses at the cuvette was measured to be of 35±5 μm (half width of $1/e^2$ maximum in irradiance). Both incident and transmitted laser pulses were monitored simultaneously using a calibrated beam splitter and two energy detectors (from Laser Precision, Rjp-735 energy probes). The detectors were linked to a computer by an IEEE interface. The linear (low-intensity) transmittance of all the samples was adjusted to 92%. Fullerene (C_{60}) dissolved in toluene ($9.02\cdot10^{-4}$ M) was used as a standard sample since its optical limiting performance had been well-documented.[18]

Acknowledgments

This work was supported by the National Natural Science Foundation of China (No. 20271036), the NSF of the Education Committee of Jiangsu Province (No. 02KJB150001), and the State Key Laboratory of Coordination Chemistry of Nanjing University in China.

[1] [1a] A. Müller, E. Diemann, R. Jostes, H. Bögge, *Angew. Chem. Int. Ed. Engl.* **1981**, *20*, 934−954. [1b] A. Müller, H. Bögge, U. Schimanski, M. Penk, K. Nieradzik, M. Dartmann, E. Krickemeyer, J. Schimanski, C. Römer, M. Römer, H. Dornfeld, U. Wienböker, W. Hellmann, *Monatsh. Chem.* **1989**, *120*,

367−391. [1c] K. E. Howard, T. B. Rauchfuss, A. L. Rheingold, *J. Am. Chem. Soc.* **1986**, *108*, 297−299. [1d] M. A. Ansari, J. A. Ibers, *Coord. Chem. Rev.* **1990**, *100*, 223−266. [1e] Y. Jeannin, F. Sèheresse, S. Bernés, F. Robert, *Inorg. Chim. Acta* **1992**, *198−200*, 493−505. [1f] X.-T. Wu, P.-C. Chen, S.-W. Du, N.-Y. Zhu, J.-X. Lu, *J. Cluster Sci.* **1994**, *5*, 265−285. [1g] R. H. Holm, *Pure Appl. Chem.* **1995**, *67*, 217−224. [1h] H.-W. Hou, X.-Q. Xin, S. Shi, *Coord. Chem. Rev.* **1996**, *153*, 25−56. [1i] D.-X. Wu, M.-C. Hong, R. Cao, H.-Q. Liu, *Inorg. Chem.* **1996**, *35*, 1080−1082. [1j] D. Coucouvanis, *Adv. Inorg. Chem.* **1998**, *45*, 1−73.

[2] [2a] R. R. Chianelli, T. A. Picoraro, T. R. Halbert, W. H. Pan, E. I. Stiefel, *J. Catal.* **1984**, *86*, 226−230. [2b] M. D. Curtis, *J. Cluster Sci.* **1996**, *7*, 247−262.

[3] [3a] R. H. Holm, *Adv. Inorg. Chem.* **1992**, *38*, 1−71. [3b] E. I. Stiefel, D. Coucouvanis, W. E. Newton (Eds.), *Molybdenum Enzymes, Cofactors and Model Systems, ACS Symposium Series 535*, American Chemical Society, Washington, DC, **1993**. [3c] E. I. Stiefel, K. Matsumoto (Eds.), *Transition Metal Sulfur Chemistry, Biological and Industrial Significance, ACS Symposium Series 653*, American Chemical Society, Washington, DC, **1996**.

[4] [4a] C.-K. Chan, C.-X. Guo, R.-J. Wang, T. C. W. Mak, C.-M. Che, *J. Chem. Soc., Dalton Trans.* **1995**, 753−757. [4b] C.-M. Che, B.-H. Xia, J.-S. Huang, C.-K. Chan, Z.-Y. Zhou, K.-K. Cheung, *Chem. Eur. J.* **2001**, *7*, 3998−4006.

[5] [5a] S. Shi, W. Ji,; S.-H. Tang, J.-P. Lang, X.-Q. Xin, *J. Am. Chem. Soc.* **1994**, *116*, 3615−3616. [5b] S. Shi, W. Ji, J.-P. Lang, X.-Q. Xin, *J. Phys. Chem.* **1994**, *98*, 3570−3572. [5c] S. Shi, W. Ji, W. Xie, T.-C. Chong, H.-C. Zeng, J.-P. Lang, X.-Q. Xin, *Mater. Chem. Phys.* **1995**, *39*, 298−303. [5d] J.-P. Lang, K. Tatsumi, H. Kawaguchi, J.-M. Lu, P. Ge, W. Ji, S. Shi, *Inorg. Chem.* **1996**, *35*, 7924−7927. [5e] H.-G. Zheng, W. Ji, M. L. K. Low, G. Sakane, T. Shibahara, X.-Q. Xin, *J. Chem. Soc., Dalton Trans.* **1997**, 2375−2362. [5f] S. Shi, in: *Optoelectronic Properties of Inorganic Compounds* (Eds. D. M. Roundhill, J. P. Fackler, Jr.), Plenum Press, New York, **1998**, pp.55−105. [5g] H. Yu, Q.-F. Xu, Z.-R. Sun, Q. Liu, J.-X. Chen, S.-J. Ji, J.-P. Lang, K. Tatsumi, *Chem. Commun.* **2001**, 2614−2615.

[6] [6a] A. Müller, M. Dartmann, C. Römer, A. Clegg, G. M. Sheldrick, *Angew. Chem. Int. Ed. Engl.* **1981**, *20*, 1060−1061. [6b] S. F. Gheller, P. A. Gazzana, A. F. Masters, R. T. C. Brownlee, M. J. O'Connor, A. G. Wedd, J. R. Rodgers, M. R. Snow, *Inorg. Chim. Acta* **1981**, *54*, L131−L132. [6c] S. F. Gheller, T. W. Hambley, J. R. Rodgers, R. T. C. Brownlee, M. J. O'Connor, M. R. Snow, A. G. Wedd, *Inorg. Chem.* **1984**, *23*, 2519−2528.

[7] [7a] H.-W. Hou, H.-G. Zheng, H. G. Ang, Y.-T. Fan, M. K. M. Low, Y. Zhu, W.-L. Wang, X.-Q. Xin, W. Ji, W.-T. Wong, *J. Chem. Soc., Dalton Trans.* **1999**, 2953−2957. [7b] C. Zhang, Y.-L. Song, Y. Xu, H. K. Fun, G.-Y. Fang, Y.-X. Wang, X.-Q. Xin, *J. Chem. Soc., Dalton Trans.* **2000**, 2823−2829.

[8] [8a] H. Kawaguchi, K. Yamada, J.-P. Lang, K. Tatsumi, *J. Am. Chem. Soc.* **1997**, *119*, 10346−10358. [8b] H. Kawaguchi, K. Tatsumi, *J. Am. Chem. Soc.* **1995**, *117*, 3885−3886.

[9] [9a] J.-P. Lang, H. Kawaguchi, S. Ohnishi, K. Tatsumi, *Chem. Commun.* **1997**, 405−406. [9b] J.-P. Lang, H. Kawaguchi, K. Tatsumi, *Inorg. Chem.* **1997**, *36*, 6447−6449. [9c] J.-P. Lang, H. Kawaguchi, S. Ohnishi, K. Tatsumi, *Inorg. Chim. Acta* **1998**, *283*, 136−142. [9d] J.-P. Lang, K. Tatsumi, *J. Organomet. Chem.* **1999**, *579*, 332−337.

[10] J.-P. Lang, K. Tatsumi, *Inorg. Chem.* **1999**, *38*, 1364−1367.

[11] [11a] A. Müller, H. Bögge, J. Schimanski, *Inorg. Chim. Acta* **1983**, *76*, L245−L246. [11b] S.-W. Du, N.-Y. Zhu, X.-T. Wu, *Polyhedron* **1992**, *11*, 2489−2493. [11c] J.-P. Lang, K. Tatsumi, *Inorg. Chem.* **1998**, *37*, 6308−6316.

[12] J.-P. Lang, K. Tatsumi, *Inorg. Chem.* **1998**, *37*, 160−162.

[13] [13a] J. M. Manoli, C. Potvin, F. Sèheresse, S. Marzak, *Inorg. Chim. Acta* **1988**, *150*, 257−268. [13b] J.-P. Lang, G.-Q. Bian, J.-H. Cai, B.-S. Kang, X.-Q. Xin, *Trans. Met. Chem.* **1995**, *20*, 376−379. [13c] M. T. Pope, J.-P. Lang, X.-Q. Xin, K.-B. Yu, *Chin. J. Chem.* **1995**, *13*, 40−46. [13d] D. T. Cromer, A. C. Larson, *Acta Crystallogr., Sect. B* **1972**, *28*, 1052−1059.

[14] K. Nilsson, A. Oskarsson, *Acta Chem. Scand.* **1982**, *36*, 605−610.

[15] Q.-F. Zhang, Y.-Y. Niu, W.-H. Leung, Y. Song, I. D. Williams, X.-Q. Xin, *Chem. Commun.* **2001**, 1126−1127.

[16] [16a] G. M. Sheldrick, *SHELXS-97, Program for the Solution of Crystal Structure*, University of Göttingen, Germany, **1997**. [16b] P. T. Beurskens, G. Admiraal, G. Beurskens, W. P. Bosman, S. Garcia-Granda, R. O. Gould, J. M. M. Smits, C. Smykalla, *PATTY, The DIRDIF Program System, Technical Report of the Crystallography Laboratory*, University of Nijmegen, The Netherlands, **1992**. [16c] P. T. Beurskens, G. Admiraal, G. Beurskens, W. P. Bosman, R. de Gelder, R. Israel, J. M. M. Smits, *DIRDIF99, The DIRDIF-99 Program System, Technical Report of the Crystallography Laboratory*, University of Nijmegen, The Netherlands, **1999**.

[17] [17a] D. T. Cromer, J. T. Waber, *International Tables for X-ray Crystallography*, Vol. IV, The Kynoch Press, Birmingham, England, Table 2.2 A, **1974**. [17b] J. A. Ibers, W. C. Hamilton, *Acta Crystallogr.* **1964**, *17*, 781−782.

[18] [18a] K. M. Nashold, D. P. Walter, *J. Opt. Soc., Am. B.* **1995**, *12*, 1228−1237. [18b] R. L. McLean, M. C. Sutherland, M. C. Brant, D. M. Brandelik, P. A. Fleitz, T. Pottenger, *Opt. Lett.* **1993**, *18*, 858−860.

Received April 10, 2003
Early View Article
Published Online October 23, 2003

